Steel and Composite Structures, *Vol. 25, No. 5 (2017) 581-591*
DOI: https://doi.org/10.12989/scs.2017.25.5.581

The dynamic instability of FG orthotropic conical shells within the SDT

Abdullah H. Sofiyev[*1], Zihni Zerin[2], Bilender P. Allahverdiev[3], David Hui[4], Ferruh Turan[2] and Hakan Erdem[5]

[1]*Department of Civil Engineering, Faculty of Engineering, Suleyman Demirel University, Isparta, Turkey*
[2]*Department of Civil Engineering, Faculty of Engineering, Ondokuz Mayis University, Samsun, Turkey*
[3]*Department of Mathematics, Faculty of Arts and Sciences, Suleyman Demirel University, Isparta, Turkey*
[4]*Department of Mechanical Engineering, University of New Orleans, New Orleans, Louisiana, USA*
[5]*Department of Civil Engineering, Faculty of Engineering, Omer Halisdemir University, Nigde, Turkey*

(*Received April 12, 2017, Revised July 22, 2017, Accepted August 05, 2017*)

Abstract. The dynamic instability of truncated conical shells subjected to dynamic axial load within first order shear deformation theory (FSDT) is examined. The conical shell is made from functionally graded (FG) orthotropic material. In the formulation of problem a dynamic version of Donnell's shell theory is used. The equations are converted to a Mathieu-Hill type differential equation employing Galerkin's method. The boundaries of main instability zones are found applying the method proposed by Bolotin. To verify these results, the results of other studies in the literature were compared. The influences of material gradient, orthotropy, as well as changing the geometric dimensions on the borders of the main areas of the instability are investigated.

Keywords: material gradient; orthotropic material; conical shells; dynamic instability; main instability zones; FSDT

1. Introduction

Most designs, regardless of their use, will be subjected to dynamic loads in their operational life. One of these structural elements is the conical shell. Increased use of conical shells in a variety of engineering applications requires the improvement of accurate theoretical models to predict their response under dynamic loads. In this sense, the solution of the dynamic instability problem of truncated cones has practical significance. Most of the existing investigation is devoted to the dynamic instability of isotropic conical shells within classical theory of shells (CST) (Kornecki 1966, Tani 1974, Tani 1976, Massalas *et al.* 1981, Bert and Birman 1988, Ganapathi *et al.* 1999, Ng *et al.* 1999, Kuntsevich and Mikhasev 2002, Qinkai and Fulei 2013, Han and Chu 2014). As the ratio of the elastic modulus to the shear modulus increases, some errors occur in the behavior of the instability of shells within the CST. For this reason, a satisfactory shear deformation theory (SDT) is required to solve of dynamic instability of composite anisotropic shells. The studies in this area are relatively few, and most of the work is dedicated the instability of homogeneous cylinders (Argento 1993, Jansen 2005, Mallon *et al.* 2010, Wosu *et al.* 2012, Neves *et al.* 2013, Akbari *et al.* 2014, Dey and Ramachandra 2014, Heydarpour *et al.* 2014, Sofiyev 2014, Su *et al.* 2014, Viola *et al.* 2014, Panda *et al.* 2015, Bhagat *et al.* 2016, Khayat *et al.* 2016, Rahmanian *et al.* 2017).

*Corresponding author, Ph.D.,
E-mail: abdullahavey@sdu.edu.tr

The modern technology requires creating new type materials that accurately describe a physical phenomenon necessary for product development and safety assessment. Recently, space, nuclear, transportation and other industries are enriched by design and development of composite, non-homogeneous and multi-functional materials. In the literature, there is sufficient research on the free vibration behavior of shells from such materials based on CST and SDT (Jansen 2005, Wosu *et al.* 2012, Neves *et al.* 2013, Akbari *et al.* 2014, Heydarpour *et al.* 2014, Najafov *et al.* 2014, Sofiyev 2014, Su *et al.* 2014, Viola *et al.* 2014, Xie *et al.* 2014, Sofiyev and Kuruoglu 2015, Ansari and Torabi 2016, Bich *et al.* 2016, Deniz *et al.* 2016, Fantuzzi *et al.* 2016, Javed *et al.* 2016, Kandasamy *et al.* 2016, Khayat *et al.* 2016, Tornabene *et al.* 2016, Vescovini and Dozio 2016, Chen *et al.* 2017b, Khayat *et al.* 2017).

The effects of shear strains are very significant on the behavior of structures consisting of FG materials. Due to the increasing importance of FG materials in planning of structures and their instability characteristics, considering combined effects of heterogeneity and shear deformations are essential. Various theories of shear deformation with the accuracy of solving instability problems are proposed, and they led to more accurate results (Ng *et al.* 2001, Yang and Shen 2003, Ansari and Darvizeh 2008, Pradyumna and Bandyopadhyay 2009, Bespalova and Urusova 2011, Ovesy and Fazilati 2012, Lei *et al.* 2014, Torki *et al.* 2014, Sofiyev 2015, Kumar *et al.* 2016, Mehri *et al.* 2016, Park *et al.* 2016, Sofiyev 2016, Sofiyev and Kuruoglu 2016, Chen *et al.* 2017a).

The above mentioned studies relate to shells composed of FG isotropic materials, and most of them considered the

Copyright © 2017 Techno-Press, Ltd.

ISSN: 1229-9367 (Print), 1598-6233 (Online)

instability of cylindrical shells and panels using various shear deformation shell theories such as first order shear deformation theory (FSDT) and higher order shear deformation theory (HSDT). The number of publications on the instability of the orthotropic and heterogeneous conical shells based on the shear deformation theories is rather limited. The purpose of this investigate is to the solution of the dynamic instability of FG orthotropic truncated conical shells within the FSDT. The expressions for the excitation frequencies of FG orthotropic cones within the FSDT are found. Finally, the influences of shear strains, material gradient, orthotropy, loading parameters, as well as the characteristics of conical shell on the main instability zones are considered in detail.

2. Basic relations

Geometry of the FG orthotropic conical shell are defined in Fig. 1, where h, L, and γ are the thickness, the slant length and the half-hill angle, respectively. R_1 and R_2 are small and large radii, and S_1 and S_2 are distances from the apex to small and large bases, respectively. The coordinate system is given as $(OS\theta z)$, in which S and θ coincides with generator and circumferential directions, respectively, and z is normal to the $S\theta$ surface.

In addition u,v,w denote displacement components in directions S,θ,z respectively, on the mid-surface, respectively. The axial load, as illustrated in Fig.1, is defined as

$$T_S^0 = -T(t) = -T_s - T_d\cos(\Gamma t),\ T_\theta^0 = 0,\ T_{S\theta}^0 = 0 \tag{1}$$

where T_S^0, T_θ^0 and $T_{S\theta}^0$ are the membrane forces, T_S is an axial load, T_d is an amplitude of dynamic axial load, Γ is the excitation frequency (in rad/s) and t is a time variable.

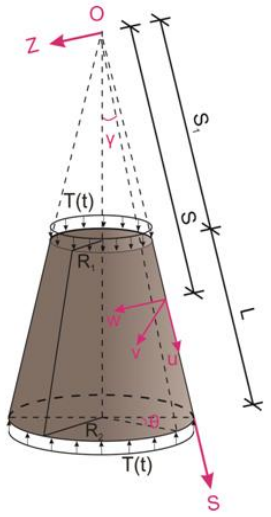

Fig. 1 FG orthotropic truncated cone subjected to dynamic axial load

The properties are assumed to have in-plane orthotropy and transverse non-homogeneity and mathematically formulated as (Massalas *et al.* 1981, Najafov *et al.* 2014, Sofiyev 2014).

$$\begin{aligned} &E_S(\bar z) = \upsilon(\bar z)E_{0S},\ E_\theta(\bar z) = \upsilon(\bar z)E_{0\theta},\\ &G_{S\theta}(\bar z) = \upsilon(\bar z)G_{0S\theta},\ G_{Sz}(\bar z) = \upsilon(\bar z)G_{0Sz},\\ &G_{\theta z}(\bar z) = \upsilon(\bar z)G_{0\theta z},\ \bar z = z/h \end{aligned} \tag{2}$$

where $E_{0S}, E_{0\theta}$ and $G_{0S\theta}, G_{0Sz}, G_{0\theta z}$ are the elasticity moduli, respectively, $\upsilon(\bar z)$ is continuous function of elasticity moduli and $\bar z$ is the normalized thickness coordinate, $-1/2 \le \bar z \le 1/2$. In additionally, the density, ρ, and Poisson′s ratios, $\nu_{S\theta}$ and $\nu_{\theta S}$, are constant. In addition, the following equality satisfied: $E_{0S}/E_{0\theta} = \nu_{S\theta}/\nu_{\theta S}$ (Ambartsumian 1964, Reddy 2004, Chen *et al.* 2017a).

In the framework of FSDT, the stress-strain relationships of shells made of FG orthotropic materials are expressed as (Sofiyev 2015, Sofiyev 2016, Sofiyev and Kuruoglu 2016)

$$\begin{bmatrix}\sigma_S\\ \sigma_\theta\\ \sigma_{\theta z}\\ \sigma_{Sz}\\ \sigma_{S\theta}\end{bmatrix} = \begin{bmatrix} K_{11}(\bar z) & K_{12}(\bar z) & 0 & 0 & 0\\ K_{21}(\bar z) & K_{22}(\bar z) & 0 & 0 & 0\\ 0 & 0 & K_{44}(\bar z) & 0 & 0\\ 0 & 0 & 0 & K_{55}(\bar z) & 0\\ 0 & 0 & 0 & 0 & K_{66}(\bar z)\end{bmatrix}\begin{bmatrix}\varepsilon_S\\ \varepsilon_\theta\\ \gamma_{\theta z}\\ \gamma_{Sz}\\ \gamma_{S\theta}\end{bmatrix} \tag{3}$$

where $\sigma_S, \sigma_\theta, \sigma_{S\theta}$ are the stresses, $\varepsilon_S, \varepsilon_\theta, \varepsilon_{S\theta}$ are the strains and the quantities for the non-homogeneous orthotropic materials, $K_{ij}(i,j=1,2,..6)$, are given as

$$\begin{aligned} &K_{11}(\bar z) = \frac{\upsilon(\bar z)E_{0S}}{1-\nu_{S\theta}\nu_{\theta S}},\ K_{22}(\bar z) = \frac{\upsilon(\bar z)E_{0\theta}}{1-\nu_{S\theta}\nu_{\theta S}},\\ &K_{12}(\bar z) = K_{21}(\bar z) = \nu_{\theta S}K_{11}(\bar z) = \nu_{S\theta}K_{22}(\bar z),\\ &K_{44}(\bar z) = \upsilon(\bar z)G_{0\theta z},\ K_{55}(\bar z) = \upsilon(\bar z)G_{0Sz},\\ &K_{66}(\bar z) = \upsilon(\bar z)G_{0S\theta}, \end{aligned} \tag{4}$$

The distributions of shear stresses within the FSTD are given as (Ambartsumian 1964, Reddy 2004, Kumar *et al.* 2016, Mehri *et al.* 2016, Sofiyev 2016, Chen *et al.* 2017a)

$$\sigma_{Sz} = \frac{df_1(z)}{dz}\phi_1(S,\theta,t) \tag{5}$$

and

$$\sigma_{\theta z} = \frac{df_2(z)}{dz}\phi_2(S,\theta,t) \tag{6}$$

where $\phi_1(S,\theta,t)$ and $\phi_2(S,\theta,t)$ are the rotations in the θz and Sz surfaces, $f_i(z), (i=1,2)$ are shear deformations functions, and varied as $f_1(z) = f_2(z) = sinh(z) - z\,cosh(1/2)$ (Timarci and Soldatos 1995, Han and Chu 2014, Sofiyev 2016).

The relationships for strains at z distance from the mid-surface of the non-homogeneous cones within the

FSDT (Sofiyev 2016)

$$\begin{bmatrix}\varepsilon_S\\ \varepsilon_\theta\\ \gamma_{S\theta}\end{bmatrix}=\begin{bmatrix} e_S - z\dfrac{\partial^2 w}{\partial S^2}\\ e_\theta - \dfrac{z}{S^2}\dfrac{\partial^2 w}{\partial \theta_1^2}+\dfrac{z}{S}\dfrac{\partial w}{\partial S}\\ \gamma_{0S\theta}-2z\left(\dfrac{1}{S}\dfrac{\partial^2 w}{\partial S\partial\theta_1}-\dfrac{1}{S^2}\dfrac{\partial w}{\partial\theta_1}\right)\end{bmatrix} + \begin{bmatrix} J_1(z)\dfrac{\partial\phi_1}{\partial S}\\ J_2(z)\dfrac{1}{S}\dfrac{\partial\phi_2}{\partial\theta_1}\\ J_1(z)\dfrac{1}{S}\dfrac{\partial\phi_1}{\partial\theta_1}+J_2(z)\dfrac{\partial\phi_2}{\partial S}\end{bmatrix} \tag{7}$$

where $\theta_1=\theta\sin\gamma$, $e_S, e_\theta, \gamma_{0S\theta}$ are mid-surface strains and the linear relationship between mid-surface strains and (u, v, w) displacements is (Yang and Shen 2003)

$$\left[e_S, e_\theta, \gamma_{0S\theta}\right]=\left[\frac{\partial u}{\partial S}, \frac{1}{S}\frac{\partial v}{\partial\theta_1}+\frac{u}{S}-\frac{w\cot\gamma}{S}, \frac{1}{S}\frac{\partial u}{\partial\theta_1}+\frac{\partial v}{\partial S}-\frac{v}{S}\right] \tag{8}$$

and the functions associated with the transverse shear stresses are expressed as

$$\begin{aligned} J_1(z)&=\int_0^z\left[\cosh(z)-\cosh(0.5)\right]/K_{55}(\bar z)dz,\\ J_2(z)&=\int_0^z\left[\cosh(z)-\cosh(0.5)\right]/K_{44}(\bar z)dz \end{aligned} \tag{9}$$

The forces and moments of inhomogeneous conical shells can be found from the following integrals (Ambartsumian 1964, Agamirov 1990, Timarci and Soldatos 1995, Reddy 2004)

$$\begin{pmatrix}T_S, T_\theta, T_{S\theta}, Q_S, Q_\theta\\ M_S, M_\theta, M_{S\theta}\end{pmatrix}=\int_{-h/2}^{h/2}\begin{pmatrix}\sigma_S, \sigma_\theta, \sigma_{S\theta}, \sigma_{Sz}, \sigma_{\theta z}\\ z\sigma_S, z\sigma_\theta, z\sigma_{S\theta}\end{pmatrix}dz \tag{10}$$

where $T_S, T_\theta, T_{S\theta}$ and $M_S, M_\theta, M_{S\theta}$ are forces and moments, and Q_S and Q_θ are shear forces.

Airy stress function, $\Phi(S,\theta,t)$, may be expressed as (Ambartsumian 1964, Agamirov 1990)

$$\left(T_S, T_\theta, T_{S\theta}\right)=h\left(\frac{1}{S^2}\frac{\partial^2\Phi}{\partial\theta_1^2}+\frac{1}{S}\frac{\partial\Phi}{\partial S}, \frac{\partial^2\Phi}{\partial S^2}, -\frac{1}{S}\frac{\partial^2\Phi}{\partial S\partial\theta_1}+\frac{1}{S^2}\frac{\partial\Phi}{\partial\theta_1}\right) \tag{11}$$

By combining the Eqs. (3), (7) and (10), one obtain relations for forces, moments and strains, then substituting the resulting relations together with expressions (11) into dynamic stability and compatibility equations (Agamirov 1990, Sofiyev 2016), one can derive basic differential equations governing equations depending on the Φ, w, ϕ_1, ϕ_2 and they expressed as

$$\begin{bmatrix} L_{11} & L_{12} & L_{13} & L_{14}\\ L_{21} & L_{22} & L_{23} & L_{24}\\ L_{31} & L_{32} & L_{33} & L_{34}\\ L_{41} & L_{42} & L_{43} & L_{44}\end{bmatrix}\begin{bmatrix}\Phi\\ w\\ \phi_1\\ \phi_2\end{bmatrix}=0 \tag{12}$$

where L_{ij} $(i, j=1,2,..,4)$ are differential operators and more details are given in the Appendix A.

The system of Eqs. (12) is the dynamic stability and compatibility equations of FG orthotropic cones within the FSDT.

3. Solution of governing equations

The FG orthotropic truncated cone is assumed to be freely supported at $S=S_1$ and $S=S_2$. The boundary conditions for the system of Eqs. (12) are written in the form (Ambartsumian 1964, Sofiyev 2015):

$$\begin{aligned} &w=0,\ M_S=0,\ \phi_2=0,\ \frac{\partial\Phi}{\partial\theta_1^2}\\ &as\ \ S=S_1\ \ and\ \ S=S_2 \end{aligned} \tag{13}$$

and the solution of system of Eqs. (12) is assumed to be

$$\begin{aligned} \Phi(S,\theta,t)&=\phi_1(t)S_2e^{(\lambda+1)\bar S}\sin(\alpha_1\bar S)\cos(\alpha_2\theta_1)\\ w(S,\theta,t)&=w_1(t)e^{\lambda\bar S}\sin(\alpha_1\bar S)\cos(\alpha_2\theta_1)\\ \phi_1(S,\theta,t)&=\bar\phi_1(t)e^{\lambda\bar S}\cos(\alpha_1\bar S)\cos(\alpha_2\theta_1)\\ \phi_2(S,\theta,t)&=\bar\phi_2(t)e^{\lambda\bar S}\sin(\alpha_1\bar S)\cos(\alpha_2\theta_1) \end{aligned} \tag{14}$$

where $\phi_1(t), w_1(t), \bar\phi_1(t), \bar\phi_2(t)$ are time dependent unknown functions, λ is a parameter that will be found from the minimizing the critical parameters, and $\bar S=\ln\frac{S}{S_2}$, $\alpha_1=\frac{m\pi}{\ln S_0}$, $\alpha_2=\frac{n}{\sin\gamma}$ in which, $S_0=\ln\frac{S_2}{S_1}$. Here m is the half wave number in the axial direction and n is the circumferential wave number.

With substituting of Eq. (14) into Eq. (12) and applying Galerkin′s method, after come simplifications, yields

$$\begin{aligned} &F_{11}\Phi_1(t)-F_{12}w_1(t)+F_{13}\bar\phi_1(t)+F_{14}\bar\phi_2(t)=0,\\ &F_{21}\Phi_1(t)-F_{22}w_1(t)+F_{23}\bar\phi_1(t)+F_{24}\bar\phi_2(t)=0,\\ &F_{31}\Phi_1(t)-F_{32}w_1(t)+F_{33}\bar\phi_1(t)+F_{34}\bar\phi_2(t)=0,\\ &F_{41}\Phi_1(t)+F_{\rho_1}\frac{d^2w_1(t)}{dt^2}-\left[T_S+T_d\cos(\Gamma t)\right]F_Tw_1(t)\\ &\qquad\qquad+F_{43}\bar\phi_1(t)+F_{44}\bar\phi_2(t)=0, \end{aligned} \tag{15}$$

where $F_{ij}(i, j=1,2,..,4)$ are parameters and more information about them are listed in Appendix B.

If omitting $\bar\Phi_1(t), \bar\phi_1(t), \bar\phi_2(t)$ from the set of Eqs. (15), after some simplifications, the following differential equation obtained as

$$\frac{d^2w_1(t)}{dt^2}+\omega_{SDT}^2\left[1-T_{s1}^{SDT}-T_{d1}^{SDT}\cos(\Gamma t)\right]w_1(t)=0 \tag{16}$$

where $T_{s1}^{SDT}=\frac{T_s}{T_{scr}^{SDT}}$ and $T_{d1}^{SDT}=\frac{T_d}{T_{scr}^{SDT}}$ are the static and dynamic axial load factors, in which T_{scr}^{SDT} is critical

static axial load (in N/m) and ω_{SDT} (in 1/s) is natural frequency for the FG orthotropic truncated cone within the FSDT and are defined as

$$T_{scr}^{SDT}=\frac{\psi_1\psi_3-\psi_2}{F_T\psi_1} \tag{17}$$

and

$$\omega_{SDT}=\sqrt{\frac{\psi_1\psi_3-\psi_2}{F_{\rho_1}\psi_1}} \tag{18}$$

wherein

$$\begin{gathered}\psi_1=\upsilon_4-\frac{\upsilon_1\upsilon_6}{\upsilon_3},\ \psi_2=\left(\upsilon_5-\frac{\upsilon_2\upsilon_6}{\upsilon_3}\right)\left(\upsilon_7-\frac{\upsilon_1\upsilon_9}{\upsilon_3}\right),\psi_3=\upsilon_8-\frac{\upsilon_2\upsilon_6}{\upsilon_3},\\ \upsilon_1=F_{21}-\frac{F_{11}F_{24}}{F_{14}},\upsilon_2=\frac{F_{12}F_{24}}{F_{14}}-F_{22},\upsilon_3=F_{23}-\frac{F_{24}F_{13}}{F_{14}},\\ \upsilon_4=F_{31}-\frac{F_{11}F_{34}}{F_{14}},\upsilon_5=\frac{F_{12}F_{34}}{F_{14}}-F_{32},\upsilon_6=F_{33}-\frac{F_{13}F_{34}}{F_{14}},\\ \upsilon_7=F_{41}-\frac{F_{11}F_{44}}{F_{14}},\upsilon_8=\frac{F_{12}F_{44}}{F_{14}},\upsilon_9=F_{43}-\frac{F_{13}F_{44}}{F_{14}}\end{gathered} \tag{19}$$

The dimensionless critical static axial load and dimensionless natural frequency of FG orthotropic truncated cones in the framework of the FSDT are defined as

$$T_{1scr}^{SDT}=\frac{T_{scr}^{SDT}}{E_{0S}} \tag{20}$$

and

$$\omega_{1SDT}=\omega_{SDT}R_1\sqrt{\frac{(1-\nu_{S\theta}^2)\rho}{E_{0S}}} \tag{21}$$

To obtain the minimum values of critical parameters within the FSDT, Eqs. (20) or (21) are minimized versus the (*m*, *n*,) and parameter λ. Magnitudes of dimensionless frequency parameter and axial buckling load of freely-supported FG orthotropic truncated conical shell using CST and FSDT are found $\lambda=1.2$ and about $\lambda=2.1$. For the freely-supported cylindrical shells are obtained at $\lambda=0$.

Note that Eq. (16) is an equation of the Mathieu Hill type. A periodic solution of this equation can be obtained applying the method proposed by Bolotin (1964). The first-order approximation to the solution with periodicity 2T can be written as

$$w_1(t)=a_1\cos\left(\frac{\Gamma t}{2}\right)+b_1\sin\left(\frac{\Gamma t}{2}\right) \tag{22}$$

where a_1 and b_1 are unknown parameters.

Substituting (22) into Eq. (16) and taking into account that a_1 and b_1 are arbitrary functions, we obtain

$$\begin{gathered}\left[-\Gamma^2+4\omega_{SDT}^2\left(1-T_{s1}-\frac{1}{2}T_{d1}\right)\right]a_1\cos\left(\frac{t\Gamma}{2}\right)\\ +\left[-\Gamma^2+4\omega_{SDT}^2\left(1-T_{s1}+\frac{1}{2}T_{d1}\right)\right]b_1\sin\left(\frac{t\Gamma}{2}\right)=0\end{gathered} \tag{23}$$

As $a_1\neq 0$ and $b_1\neq 0$, from Eq. (23), the formula for the boundaries of main instability zones of FG orthotropic truncated cones within the FSDT is obtained as

$$\Gamma_{1j}^{SDT}=2\omega_{SDT}\sqrt{1-T_{s1}\mp\frac{1}{2}T_{d1}},\ (j=1,2) \tag{24}$$

where $\Gamma_{1j}^{SDT}(j=1,2)$ are the borders of main instability zones based on the FSDT, sign (-) and (+) is used, as $j=1$ and 2, respectively, and the following definition applies

$$\overline{\Gamma}_{1j}^{SDT}=2\pi R_1\Gamma_{1j}^{SDT}\sqrt{\frac{(1-\nu_{S\theta}^2)\rho}{E_{0S}}},\ (j=1,2) \tag{25}$$

By using Eqs. (24) and (25) will be determined the borders of main instability zones of FG orthotropic truncated cones within the FSDT.

As neglecting the dynamic axial load factor from Eq. (24), the expression for the point of origin of main instability zones of inhomogeneous orthotropic cones within the FSDT, in the special case.

As neglecting the shear stresses effects from Eq. (24), the expressions for borders of main instability zones of inhomogeneous orthotropic truncated conical shells within the CST are obtained.

4. Numerical analysis

4.1 Comparative study

In Table 1, the magnitudes of $\overline{\Gamma}_{1j}^{CST}(j=1,2)$, with various T_{d1} and circumferential wave numbers compared with the results of Ng *et al.* (1998) for isotropic cylinders. In the comparison $\upsilon(\bar{z})=1$, $E_{0S}=E_{0\theta}=E_0$, $\nu_{12}=\nu_{21}=\nu_0$ and $\gamma\to 0^o$, $R_1\approx R_2=R$, $L=L_1$, should be taken into account in (24) and (25), as well as the shear stresses were not considered. Here the radius of cylinder is R and the length is L_1. The static axial load factor is $T_{s1}=1/10$, the computations parameters are considered as, $h=0.01m$; $R/h=100$; $L/h=200$ and $E_0=2.1\times 10^{11}Pa$, $\nu_0=0.3$, $\rho=8000kg/m^3$.

Comparisons show that the results are in harmony.

The magnitudes of $\overline{\omega}_1=\omega R_1\sqrt{(1-\nu_0^2)\rho/E_0}$ for H isotropic conical shell are compared with the results of Han and Chu (2014), and Lam and Hua (1999) for different L/R_2 and are given in Table 2. If the transverse shear stresses are not considered and $\upsilon(\bar{z})=1$, $E_{0S}=E_{0\theta}=E_0$, $\nu_{S\theta}=\nu_{\theta S}=\nu_0$ considered in Eq. (21), as well as the shear stresses were not considered, it is turn into the expression for the homogeneous isotropic cones based on the CST. The input parameters of the homogeneous isotropic truncated conical shell are considered as,

Table 1 Comparison of magnitudes of borders of main instability zones, $\overline{\Gamma}_{1j}^{CST}(j=1,2)$, for isotropic cylindrical shell

	n =3				n =4			
	Ng *et al.* (1998)		Present study		Ng *et al.* (1998)		Present study	
T_{d1}	$\overline{\Gamma}_{11}^{CST}$	$\overline{\Gamma}_{12}^{CST}$	$\overline{\Gamma}_{11}^{CST}$	$\overline{\Gamma}_{12}^{CST}$	$\overline{\Gamma}_{11}^{CST}$	$\overline{\Gamma}_{12}^{CST}$	$\overline{\Gamma}_{11}^{CST}$	$\overline{\Gamma}_{12}^{CST}$
0	0.3862	0.3862	0.3945	0.3945	0.2572	0.2572	0.2621	0.2621
0.1	0.3859	0.3865	0.3934	0.3956	0.2566	0.2576	0.2614	0.2629
0.3	0.3855	0.3867	0.3923	0.3967	0.2561	0.2581	0.2607	0.2636

Table 2 Comparison of $\overline{\omega}_1$ for homogenous isotropic conical shells for different L/R_2

	$L/R_2=0.5$		$L/R_2=1$	
n	Lam and Hua (1999)	Present study	Han and Chu (2014)	Present study
3	0.7376	0.7507	0.4205	0.4369
4	0.6362	0.6470	0.3067	0.3088
5	0.5528	0.5606	0.2646	0.2579
6	0.4950	0.5002	0.2750	0.2647
7	0.4661	0.4695	0.3164	0.3102
8	0.4660	0.4682	-	0.3798
9	0.4916	0.4931	-	0.4660

$\nu_0=0.3,\ h/R_2=0.01,\ \gamma=30^\circ$. As can be seen from Table 2, our results are in good agreement, as a rule, with the results of Han and Chu (2014) and Lam and Hua (1999) for different L/S_2.

The magnitudes of $\omega_{1SDT}=\omega_{SDT}(L_1^2/h)\sqrt{\rho/E_{0\theta}}$ for cylindrical shells made of orthotropic materials using FSDT and compared with the results of Timarci and Soldatos (1995) (Table 3). The dimensionless frequency parameters of cylindrical shells are presented for hyperbolic cosine function of shear deformation functions as Timarci and Soldatos (1995): $\phi_1(z)=\phi_2(z)=h\sinh(\bar{z})-z\cosh(0.5)$. In the comparison, $\upsilon(\bar{z})=1,\ \gamma\to 0^o,\ R_1\approx R_2=R$ and $L=L_1$ should be taken into account in (18), the formula for ω_{1SDT} of the homogenous orthotropic cylindrical shell are obtained. The orthotropic material properties are taken to be $E_{0S}/E_{0\theta}=25;\ G_{0S\theta}/E_{0\theta}=G_{0Sz}/E_{0\theta}=0.5;\ G_{0\theta z}=0.2E_{0\theta};$ $\nu_{S\theta}=0.25;\ \rho=1$ and $L_1/h=100$. In Table 3, the circumferential wave number corresponding to the minimum values of the frequency parameters is given in parentheses, in the present study. It is evident from the Table 3 that very good agreement has been achieved.

Table 3 Comparison of ω_{1SDT}, for [0/90]S cylinders made of orthotropic material within the FSDT

R/L_1	Timarci and Soldatos (1995)	Present study
5	19.989	20.054(18)
10	16.492	16.534(28)
20	14.772	14.808(43)
50	13.825	13.859(71)

4.2 Influences of shear strains and material gradient on the boundaries of main instability zones of orthotropic conical shells

In this subsection, new computations were presented to investigate the effects of shear strains and material gradient on the boundaries of main instability zones using Eqs. (23) and (24). The material properties vary trough the thickness direction with linear and quadratic functions, i.e., $\upsilon(\bar{z})=1+\mu\bar{z}^k\ (k=1,2)$, in which μ is a material gradient parameter, satisfying $0\le\mu\le 1$. Obviously, as the $\mu=0$, the FG orthotropic material becomes a homogeneous (H) orthotropic material (Sofiyev 2014). In the all figures, FG-linear and FG- quadratic functions are given as FG-L and FG-Q. The truncated conical shells made of boron/epoxy, in which material are considered as, $E_{0S}=2.069\times10^{11}Pa,\ E_{0\theta}=2.069\times10^{10}Pa,\ G_{0S\theta}=6.9\times10^{9}Pa,$ $G_{0Sz}=6.9\times10^{9}Pa,\ G_{0\theta z}=4.14\times10^{9}Pa,\ \nu_{\theta S}/\nu_{S\theta}=E_{0\theta}/E_{0S},$ $\nu_{S\theta}=0.3$ and $\rho=1950kg/m^3$ (Reddy 2004).

The influences of material gradient and shear stresses on the boundaries of main instability zones of orthotropic conical shells for different R_1/h are plotted in Fig. 2. The geometry of orthotropic conical shells are considered as, $R_1/L=5,\ \gamma=30^o$ and $T_{s1}=0.1,\ T_{d1}=0,0.1,0.3,0.5$ $m=1$ and $n=3$. The magnitudes of borders of main instability areas for FG and H orthotropic cones diminish considerable, as the R_1/h increment, whereas, these magnitudes decrease little, as T_{d1} increment.

If the magnitudes of $\overline{\Gamma}_{1j}^{SDT}$ and $\overline{\Gamma}_{1j}^{CST}(j=1,2)$ are compared to each other, the difference between them reduce from 40.7% to 11.7%, 39% to 10.97% and 42.57% to

12.75%, when R_1/h increment from 20 to 50, respectively. The influences of material gradient on the magnitudes of boundaries of main instability zones for FG-L and FG-Q orthotropic cones based on the CST remain constant (4.2%) and (7.2%), whereas, those based on the FSDT increment from 1.85% to 3.3% and from 3.77% to 5.91%.

The effect of L/R_1, on the magnitudes of borders of main instability zones of FG and H orthotropic cones on the basis of FSDT and CST for mode (1,4) are shown in Fig. 3.

The calculations data are considered as, $\gamma = 30^o$, $R_1/h = 25$, $L/R_1 = 2$, and $T_{s1} = 0.2$. The magnitudes of borders of main instability zones of truncated cones reduce, as the L/R_1 increases from 0.3 to 0.5. As the magnitudes of borders of main instability zones for homogeneous, FG-L and FG-Q orthotropic cones within the FSDT are compared with those of CST, the influences of shear strains on the borders of main instability zones diminish from 18.42% to 6.79%, 17.35% to 6.24% and 19.84% to 7.53%, when L/R_1 varies between 0.3 and 0.5, respectively.

The influences of FG-L and FG-Q compositional on the magnitudes of borders of instability zones for orthotropic truncated cones within the CST decrease from 4.14% to 3.73%, from 7.15% to 6.86%, while these influences within the FSDT increase from 2.88% to 3.16% and from 5.29% to 6.04%, respectively. The effect of shear stresses appears to reduce the effect of material gradient on the size of the boundaries of the main unstable zones.

The effects of the half-hill angle, γ, on the magnitudes of borders of main instability zones of FG and H orthotropic shells for mode (1,2) are shown in Fig. 4. The calculations data are, $\gamma = 30^o$, $R_1/h = 30$, $L/R_1 = 0.3$ and $T_{s1} = 0.1$. It is obvious that the magnitudes of borders of main instability zones of truncated cones diminish very little, as the half-hill angle, γ, increases from 30^o to 60^o. As the magnitudes of borders of main instability zones for homogeneous, FG-L and FG-Q orthotropic cones within the FSDT are compared with those of CST, the influences of shear stresses on the boundaries of main instability zones remain constant 13.47%, 12.6% and 14.6%, respectively, when the half-hill angle, γ, increases from30^o to 60^o.

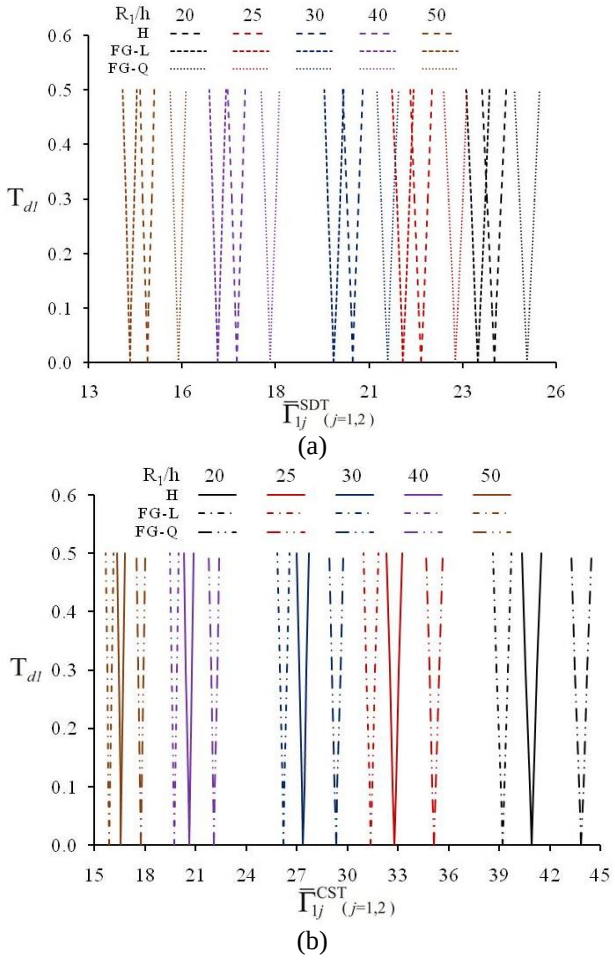

Fig. 2 Effect of non-homogeneity on the borders of main instability areas of orthotropic conical on the basis of (a) FSDT and (b) CST for different R_1/h

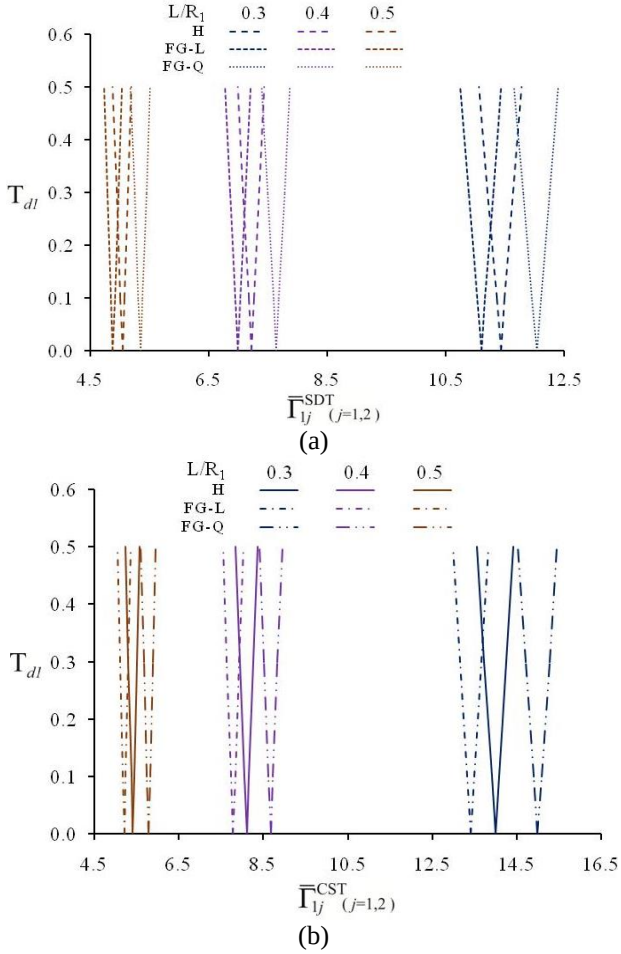

Fig. 3 Influence of the material gradient on the borders of main instability areas of orthotropic conical shells within the (a) FSDT and (b) CST for different L/R_1

The influences of FG-L and FG-Q orthotropic compositions on the magnitudes of boundaries of main instability zones for truncated cones within the CST increase from 4.04% to 4.19%, from 7.09% to 7.19%, while these influences within the FSDT increase from 3.08% to 3.22 % and from 5.65% to 5.73% respectively.

Fig. 5 depict the effects of the ratio, $E_{0S}/E_{0\theta}$, on the $\overline{\Gamma}_{1j}^{SDT}$ and $\overline{\Gamma}_{1j}^{CST}(j=1,2)$ of H and FG orthotropic cones. The cones data are, $\gamma=45^{o}$, $R_1=25h$, $L=0.2R_1$, and (m,n)=(1,1). The axial static load factor is taken to be $T_{s1}=0.1$. The material properties are taken to be $E_{0S}/E_{0\theta}=5;15;25$, $G_{0S\theta}/E_{0\theta}=G_{0Sz}/E_{0\theta}=0.5$, $G_{0\theta z}/E_{0\theta}=0.6$, $\nu_{S\theta}=0.25$ and $\rho=1950\,kg/m^3$. It is obvious that the magnitudes of borders of main instability zones of truncated cones diminish with increasing of $E_{0S}/E_{0\theta}$ from 5 to 25.

The sizes of main instability zones diminish, while the influences of material gradient on the magnitudes of borders of main instability zones nearly remain constant, when $E_{0S}/E_{0\theta}$ increases.

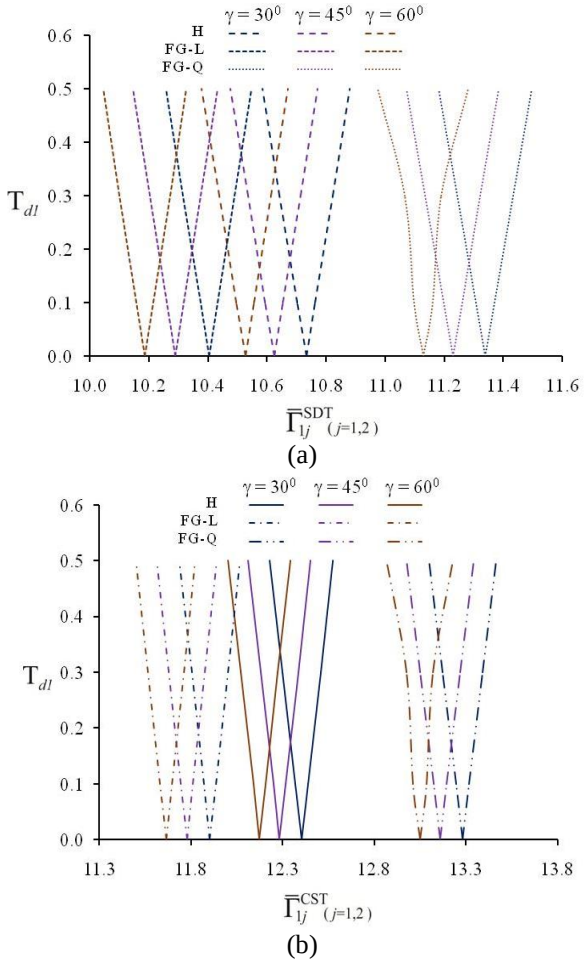

Fig. 4 Influence of the material gradient on the borders of main instability zones of orthotropic conical within the (a) FSDT and (b) CST for different the half-hill angle, γ

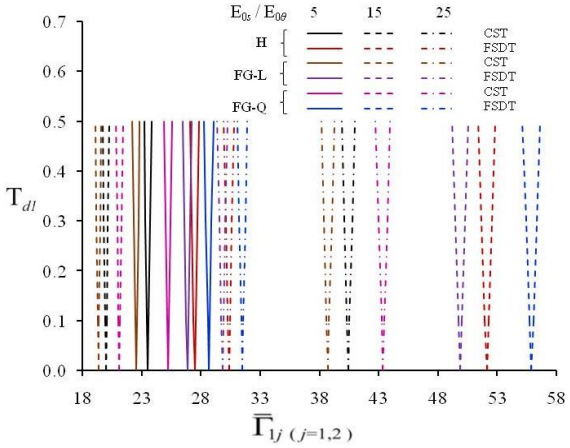

Fig. 5 Influence of material gradient on the borders of main instability areas of orthotropic conical shells within FSDT and CST for different orthotropy ratio, $E_{0S}/E_{0\theta}$

As can be seen that the influences of shear strains on the boundaries of main instability zones for H, FG-L and FG-Q orthotropic cones increase from 15.057% to 41.73%, from 14.14% to 40.25% and from 16.28% to 43.64%, respectively, when $E_{0S}/E_{0\theta}$ varies between 5 and 25. It is shown that the influences of FG-L and FG-Q orthotropic profiles on the magnitudes of boundaries of main instability zones for truncated cones within the CST vary between 4.21% and 4.25%, 7.21% and 7.31%, while these influences within the FSDT decrease from 3.19% to 1.82 % and from 5.66% to 3.71%, respectively.

5. Conclusions

The dynamic instability of truncated conical shells subjected to dynamic axial load within the FSDT is examined. The conical shell is made from FG and orthotropic material. In the formulation of problem a dynamic version of Donnell's shell theory is used. The equations are converted to a Mathieu-Hill type differential equation employing Galerkin′s method. The boundaries of main instability zones are found by using Bolotin method. To verify these results, the results of other studies in the literature were compared.

The numerical results support the following conclusions:

a) The influences of material gradient on the magnitudes of boundaries of main instability zones for FG-L and FG-Q orthotropic cones based on the CST remain constant, whereas, those based on the FSDT increases, as R_1/h increment.

b) The effect of shear stresses appears to reduce the effect of material gradient on the size of the boundaries of main unstable zones.

c) The influences of shear strains on the borders of main instability zones for FG-L and FG-Q orthotropic cones diminish, when L/R_1 varies between 0.3 and 0.5.

d) The influences of shear stresses on the boundaries of main instability zones for FG-L and FG-Q orthotropic cones remain constant when the half-hill angle, γ, increases from 30^o to 60^o.

e) The influences of shear strains on the boundaries of main instability zones for FG-L and FG-Q orthotropic cones increase, when $E_{0S}/E_{0\theta}$ varies between 5 and 25.

References

Agamirov, V. (1990), "Dynamic problems of nonlinear shells theory", Science Edition, Moscow.

Akbari, M., Kiani, Y., Aghdam, M. and Eslami, M. (2014), "Free vibration of FGM Lévy conical panels", *Compos. Struct.*, **116**, 732-746.

Ambartsumian, S.A. (1964), Theory of anisotropic plates: strength, stability, vibration, Technomic Publishing Company, Stamford, USA.

Ansari, R. and Darvizeh, M. (2008), "Prediction of dynamic behaviour of FGM shells under arbitrary boundary conditions", *Compos. Struct.*, **85**(4), 284-292.

Ansari, R. and Torabi, J. (2016), "Numerical study on the buckling and vibration of functionally graded carbon nanotube-reinforced composite conical shells under axial loading", *Composites Part B: Eng*., **95**, 196-208.

Argento, A. (1993), "Dynamic stability of a composite circular cylindrical shell subjected to combined axial and torsional loading", *J. Compos. Mater*., **27**(18), 1722-1738.

Bert, C.W. and Birman, V. (1988), "Parametric instability of thick, orthotropic, circular cylindrical shells", *Acta Mech*., **71**(1-4), 61-76.

Bespalova, E. and Urusova, G. (2011), "Identifying the domains of dynamic instability for inhomogeneous shell systems under periodic loads", *Int. Appl. Mech*., **47**(2), 186-194.

Bhagat, V.S., Pitchaimani, J. and Murigendrappa, S. (2016), "Buckling and dynamic characteristics of a laminated cylindrical panel under non-uniform thermal load", *Steel Compos. Struct.*, **22**(6), 1359-1389.

Bich, D.H., Ninh, D.G., Kien, B.H. and Hui, D. (2016), "Nonlinear dynamical analyses of eccentrically stiffened functionally graded toroidal shell segments surrounded by elastic foundation in thermal environment", *Composites Part B: Eng*., **95**, 355-373.

Bolotin, V. (1964), Dynamic stability of elastic systems, Holden-Day, San Francisco.

Chen, C.S., Liu, F.H. and Chen, W.R. (2017a), "Dynamic characteristics of functionally graded material sandwich plates in thermal environments", *Mech. Adv. Mater. Struct*., **24**(2), 157-167.

Chen, C.S., Liu, F.H. and Chen, W.R. (2017b), "Vibration and stability of initially stressed sandwich plates with FGM face sheets in thermal environments", *Steel Compos. Struct*, **23**(3), 251-261.

Deniz, A., Zerin, Z. and Karaca, Z. (2016), "Winkler-Pasternak foundation effect on the frequency parameter of FGM truncated conical shells in the framework of shear deformation theory", *Composites Part B: Eng*., **104**, 57-70.

Dey, T. and Ramachandra, L. (2014), "Static and dynamic instability analysis of composite cylindrical shell panels subjected to partial edge loading", *Int. J. Nonlinear Mech*., **64**, 46-56.

Fantuzzi, N., Brischetto, S., Tornabene, F. and Viola, E. (2016), "2D and 3D shell models for the free vibration investigation of functionally graded cylindrical and spherical panels", *Compos. Struct*., **154**, 573-590.

Ganapathi, M., Patel, B., Sambandam, C. and Touratier, M. (1999), "Dynamic instability analysis of circular conical shells", *Compos. Struct*., **46** (1), 59-64.

Han, Q. and Chu, F. (2014), "Parametric resonance of truncated conical shells rotating at periodically varying angular speed", *J. Sound Vib*., **333**(13), 2866-2884.

Heydarpour, Y., Malekzadeh, P. and Aghdam, M. (2014), "Free vibration of functionally graded truncated conical shells under internal pressure", *Meccanica*, **49**(2), 267-282.

Jansen, E.L. (2005), "Dynamic stability problems of anisotropic cylindrical shells via a simplified analysis", *Nonlinear Dynam*., **39** (4), 349-367.

Javed, S., Viswanathan, K. and Aziz, Z. (2016), "Free vibration analysis of composite cylindrical shells with non-uniform thickness walls", *Steel Compos. Struct*., **20**(5), 1087-1102.

Kandasamy, R., Dimitri, R. and Tornabene, F. (2016), "Numerical study on the free vibration and thermal buckling behavior of moderately thick functionally graded structures in thermal environments", *Compos. Struct.*, **157**, 207-221.

Khayat, M., Poorveis, D. and Moradi, S. (2016), "Buckling analysis of laminated composite cylindrical shell subjected to lateral displacement-dependent pressure using semi-analytical finite strip method", *Steel Compos. Struct*., **22**(2), 301-321.

Khayat, M., Poorveis, D. and Moradi, S. (2017), "Buckling analysis of functionally graded truncated conical shells under external displacement-dependent pressure", *Steel Compos. Struct*., **23**(1), 1-16.

Kornecki, A. (1966), "Dynamic stability of truncated conical shells under pulsating pressure(Parametric vibrations determining dynamic stability of simply supported truncated conical shells under pulsating pressure)", *Israel J. Technol*., **4**, 110-120.

Kumar, R., Dutta, S. and Panda, S. (2016), "Linear and non-linear dynamic instability of functionally graded plate subjected to non-uniform loading", *Compos. Struct*., **154**, 219-230.

Kuntsevich, S. and Mikhasev, G. (2002), "Local parametric vibrations of a noncircular conical shell subjected to nonuniform pulsating pressure", *Mech. Solids*, **37**(3), 134-139.

Lam, K. and Hua, L. (1999), "Influence of boundary conditions on the frequency characteristics of a rotating truncated circular conical shell", *J. Sound Vib*., **223**(2), 171-195.

Lei, Z., Zhang, L., Liew, K. and Yu, J. (2014), "Dynamic stability analysis of carbon nanotube-reinforced functionally graded cylindrical panels using the element-free kp-Ritz method", *Compos. Struct*., **113**, 328-338.

Mallon, N., Fey, R. and Nijmeijer, H. (2010), "Dynamic stability of a base-excited thin orthotropic cylindrical shell with top mass: simulations and experiments", *J. Sound Vib*., **329**(15), 3149-3170.

Massalas, C., Dalamangas, A. and Tzivanidis, G. (1981), "Dynamic instability of truncated conical shells, with variable modulus of elasticity, under periodic compressive forces", *J. Sound Vib*., **79**(4), 519-528.

Mehri, M., Asadi, H. and Wang, Q. (2016), "On dynamic instability of a pressurized functionally graded carbon nanotube reinforced truncated conical shell subjected to yawed supersonic airflow", *Compos. Struct*., **153**, 938-951.

Najafov, A., Sofiyev, A., Hui, D., Karaca, Z., Kalpakci, V. and Ozcelik, M. (2014), "Stability of EG cylindrical shells with shear stresses on a Pasternak foundation", *Steel Compos. Struct*., **17**, 453-470.

Neves, A., Ferreira, A., Carrera, E., Cinefra, M., Roque, C., Jorge, R. and Soares, C. (2013), "Free vibration analysis of functionally graded shells by a higher-order shear deformation theory and radial basis functions collocation, accounting for through-the-thickness deformations", *Eur. J. Mech. - A - Solids*, **37**, 24-34.

Ng, T., Hua, L., Lam, K. and Loy, C. (1999), "Parametric instability of conical shells by the generalized differential quadrature method", *Int. J. Numer. Meth. Eng*., **44**(6), 819-837.

Ng, T., Lam, K. and Reddy, J. (1998), "Parametric resonance of a

rotating cylindrical shell subjected to periodic axial loads", *J. Sound Vib.*, **214**(3), 513-529.
Ng, T., Lam, K., Liew, K. and Reddy, J. (2001), "Dynamic stability analysis of functionally graded cylindrical shells under periodic axial loading", *Int. J. Solids Struct.*, **38**(8), 1295-1309.
Ovesy, H. and Fazilati, J. (2012), "Parametric instability analysis of moderately thick FGM cylindrical panels using FSM", *Comput. Struct.*, **108**, 135-143.
Panda, H., Sahu, S. and Parhi, P. (2015), "Hygrothermal response on parametric instability of delaminated bidirectional composite flat panels", *Eur. J. Mech. - A - Solids*, **53**, 268-281.
Park, W.T., Han, S.C., Jung, W.Y. and Lee, W.H. (2016), "Dynamic instability analysis for S-FGM plates embedded in Pasternak elastic medium using the modified couple stress theory", *Steel Compos. Struct.*, **22**(6), 1239-1259.
Pradyumna, S. and Bandyopadhyay, J. (2009), "Dynamic instability of functionally graded shells using higher-order theory", *J. Eng. Mech.*, **136**(5), 551-561.
Qinkai, H. and Fulei, C. (2013), "Parametric instability of a rotating truncated conical shell subjected to periodic axial loads", *Mech. Res. Commun.*, **53**, 63-74.
Rahmanian, M., Firouz-Abadi, R. and Cigeroglu, E. (2017), "Dynamics and stability of conical/cylindrical shells conveying subsonic compressible fluid flows with general boundary conditions", *Int. J. Mech.Sci.*, **120**, 42-61.
Reddy, J.N. (2004), Mechanics of laminated composite plates and shells: theory and analysis, CRC press.
Sofiyev, A. (2014), "The combined influences of heterogeneity and elastic foundations on the nonlinear vibration of orthotropic truncated conical shells", *Composites Part B: Eng.*, **61**, 324-339.
Sofiyev, A. (2015), "Influences of shear stresses on the dynamic instability of exponentially graded sandwich cylindrical shells", *Composites Part B: Eng.*, **77**, 349-362.
Sofiyev, A. (2016), "Parametric vibration of FGM conical shells under periodic lateral pressure within the shear deformation theory", *Composites Part B: Eng.*, **89**, 282-294.
Sofiyev, A. and Kuruoglu, N. (2015), "Buckling of non-homogeneous orthotropic conical shells subjected to combined load", *Steel Compos. Struct.*, **19**(1), 1-19.
Sofiyev, A. and Kuruoglu, N. (2016), "Domains of dynamic instability of FGM conical shells under time dependent periodic loads", *Compos. Struct.*, **136**, 139-148.
Su, Z., Jin, G. and Ye, T. (2014), "Three-dimensional vibration analysis of thick functionally graded conical, cylindrical shell and annular plate structures with arbitrary elastic restraints", *Compos. Struct.*, **118**, 432-447.
Tani, J. (1974), "Dynamic instability of truncated conical shells under periodic axial load", *Int. J. Solids Struct.*, **10**(2), 169-176.
Tani, J. (1976), "Influence of deformations prior to instability on the dynamic instability of conical shells under periodic axial load", *J. Appl. Mech.*, **43**(1), 87-91.
Timarci, T. and Soldatos, K. (1995), "Comparative dynamic studies for symmetric cross-ply circular cylindrical shells on the basis of a unified shear deformable shell theory", *J. Sound Vib.*, **187**(4), 609-624.
Torki, M.E., Kazemi, M.T., Reddy, J.N., Haddadpoud, H. and Mahmoudkhani, S. (2014), "Dynamic stability of functionally graded cantilever cylindrical shells under distributed axial follower forces", *J. Sound Vib.*, **333**(3), 801-817.
Tornabene, F., Fantuzzi, N. and Bacciocchi, M. (2016), "The GDQ method for the free vibration analysis of arbitrarily shaped laminated composite shells using a NURBS-based isogeometric approach", *Compos. Struct.*, **154**, 190-218.
Vescovini, R. and Dozio, L. (2016), "A variable-kinematic model for variable stiffness plates: Vibration and buckling analysis", *Compos. Struct.*, **142**, 15-26.
Viola, E., Rossetti, L., Fantuzzi, N. and Tornabene, F. (2014), "Static analysis of functionally graded conical shells and panels using the generalized unconstrained third order theory coupled with the stress recovery", *Compos. Struct.*, **112**, 44-65.
Wosu, S., Hui, D. and Daniel, L. (2012), "Hygrothermal effects on the dynamic compressive properties of graphite/epoxy composite material", *Composites Part B: Eng.*, **43**(3), 841-855.
Xie, X., Jin, G., Ye, T. and Liu, Z. (2014), "Free vibration analysis of functionally graded conical shells and annular plates using the Haar wavelet method", *Appl. Acoust.*, **85**, 130-142.
Yang, J. and Shen, H.S. (2003), "Free vibration and parametric resonance of shear deformable functionally graded cylindrical panels", *J. Sound Vib.*, **261**(5), 871-893.

CC

Appendix A

where $L_{ij}(i,j=1,2,\ldots 4)$ are differential operators and are given as

$$L_{11}=a_{12}h\frac{\partial^4}{\partial S^4}+\frac{(a_{11}-a_{31})h}{S^2}\frac{\partial^4}{\partial S^2\partial\theta_1^2}+\frac{(3a_{31}-a_{21}-3a_{11})h}{S^3}\frac{\partial^3}{\partial S\,\partial\theta_1^2}+\frac{(a_{11}+a_{12}-a_{22})h}{S}\frac{\partial^3}{\partial S^3}+\frac{(a_{22}-a_{12}-a_{11}-a_{21})h}{S^2}\frac{\partial^2}{\partial S^2}+\frac{3(a_{21}+a_{11}-a_{31})h}{S^4}\frac{\partial^2}{\partial\theta_1^2}+\frac{2a_{21}h}{S^3}\frac{\partial}{\partial S}$$

$$L_{12}=-a_{13}\frac{\partial^4}{\partial S^4}-\frac{(a_{14}+a_{32})}{S^2}\frac{\partial^4}{\partial S^2\partial\theta_1^2}+\frac{3(a_{14}+a_{32})+a_{24}}{S^3}\frac{\partial^3}{\partial S\,\partial\theta_1^2}-\frac{a_{13}+a_{14}-a_{23}}{S}\frac{\partial^3}{\partial S^3}+\frac{(a_{13}+a_{14}-a_{23}+a_{24})}{S^2}\frac{\partial^2}{\partial S^2}-\frac{3(a_{14}+a_{24}+a_{32})}{S^4}\frac{\partial^2}{\partial\theta_1^2}-\frac{2a_{24}}{S^3}\frac{\partial}{\partial S}$$

$$L_{13}=a_{15}\frac{\partial^3}{\partial S^3}+\frac{(a_{15}-a_{25})}{S}\frac{\partial^2}{\partial S^2}+\frac{a_{35}}{S^2}\frac{\partial^3}{\partial S\partial\theta_1^2}-J_3\frac{\partial}{\partial S}-\frac{(a_{15}-a_{25})}{S^2}\frac{\partial}{\partial S}-\frac{a_{35}}{S^3}\frac{\partial^2}{\partial\theta_1^2}$$

$$L_{14}=\frac{(a_{18}+a_{38})}{S}\frac{\partial^3}{\partial S^2\partial\theta_1}-\frac{(a_{18}+a_{28}+a_{38})}{S^2}\frac{\partial^2}{\partial S\partial\theta_1}+\frac{2a_{28}}{S^3}\frac{\partial}{\partial\theta_1},$$

$$L_{21}=\frac{a_{21}h}{S^3}\frac{\partial^4}{\partial\theta_1^4}+\frac{(a_{22}-a_{31})h}{S}\frac{\partial^4}{\partial S^2\partial\theta_1^2}+\frac{a_{21}h}{S^2}\frac{\partial^3}{\partial S\partial\theta_1^2}$$

$$L_{22}=-\frac{(a_{32}+a_{23})}{S}\frac{\partial^4}{\partial S^2\partial\theta_1^2}-\frac{a_{24}}{S^2}\frac{\partial^3}{\partial S\partial\theta_1^2}-\frac{a_{24}}{S^3}\frac{\partial^4}{\partial\theta_1^4},\ L_{23}=\frac{(a_{25}+a_{35})}{S}\frac{\partial^3}{\partial S\partial\theta_1^2}+\frac{a_{35}}{S^2}\frac{\partial^2}{\partial\theta_1^2}$$

$$L_{24}=a_{38}\frac{\partial^3}{\partial S^2\partial\theta_1}+\frac{2a_{38}}{S}\frac{\partial^2}{\partial S\partial\theta_1}+\frac{a_{28}}{S^2}\frac{\partial^3\psi}{\partial\theta_1^3}-J_4\frac{\partial}{\partial\theta_1}$$

$$L_{31}=\frac{b_{11}h}{S^4}\frac{\partial^4}{\partial\theta_1^4}+\frac{(2b_{31}+b_{21}+b_{12})h}{S^2}\frac{\partial^4}{\partial S^2\partial\theta_1^2}-\frac{2(b_{31}+b_{21})h}{S^3}\frac{\partial^3}{\partial S\partial\theta_1^2}+\frac{2(b_{31}+b_{21}+b_{11})h}{S^4}\frac{\partial^2}{\partial\theta_1^2}+\frac{b_{11}h}{S^3}\frac{\partial}{\partial S}-\frac{b_{11}h}{S^2}\frac{\partial^2}{\partial S^2}+\frac{(b_{21}+2b_{22}-b_{12})h}{S}\frac{\partial^3\Phi}{\partial S^3}+b_{22}h\frac{\partial^4}{\partial S^4}$$

$$L_{32}=-\frac{b_{14}}{S^4}\frac{\partial^4}{\partial\theta_1^4}+\frac{2b_{32}-b_{13}-b_{24}}{S^2}\frac{\partial^4}{\partial S^2\partial\theta_1^2}+\frac{2(b_{24}-b_{32})}{S^3}\frac{\partial^3}{\partial S\partial\theta_1^2}+\frac{2(b_{32}-b_{24}-b_{14})}{S^4}\frac{\partial^2}{\partial\theta_1^2}-\frac{b_{14}}{S^3}\frac{\partial}{\partial S}+\left(\frac{b_{14}}{S^2}+\frac{\cot\gamma}{S}\right)\frac{\partial^2}{\partial S^2}+\frac{b_{13}-b_{24}-2b_{23}}{S}\frac{\partial^3}{\partial S^3}-b_{23}\frac{\partial^4}{\partial S^4}$$

$$L_{33}=\frac{(2b_{35}+b_{15})}{S^2}\frac{\partial^3}{\partial S\partial\theta_1^2}+b_{25}\frac{\partial^3}{\partial S^3}+\frac{(2b_{25}-b_{15})}{S}\frac{\partial^2}{\partial S^2},$$

$$L_{34}=\frac{b_{18}}{S^3}\frac{\partial^3}{\partial\theta_1^3}+\frac{(2b_{38}+b_{28})}{S}\frac{\partial^3}{\partial S^2\partial\theta_1}+\frac{(2b_{38}-b_{18})}{S^2}\frac{\partial^2}{\partial S\partial\theta_1}+\frac{b_{18}}{S^3}\frac{\partial}{\partial\theta_1}$$

$$L_{41}=\frac{h\cot\gamma}{S}\frac{\partial^2}{\partial S^2},\ L_{42}=-T(t)\frac{\partial^2}{\partial S^2},\ L_{43}=J_3\left(\frac{\partial}{\partial S}+\frac{1}{S}\right),\ L_{44}=\frac{J_4}{S}\frac{\partial}{\partial\theta_1},\quad \text{(A1)}$$

where

$a_{11}=\Pi_{11}^1b_{11}+\Pi_{12}^1b_{21}$, $a_{12}=\Pi_{11}^1b_{12}+\Pi_{12}^1b_{22}$, $a_{13}=\Pi_{11}^1b_{13}+\Pi_{12}^1b_{23}+\Pi_{11}^2$, $a_{14}=\Pi_{11}^1b_{14}+\Pi_{12}^1b_{24}+\Pi_{12}^2$,
$a_{15}=\Pi_{11}^1b_{15}+\Pi_{12}^1b_{25}+\Pi_{15}^1$, $a_{18}=\Pi_{11}^1b_{18}+\Pi_{12}^1b_{28}+\Pi_{18}^1$, $a_{21}=\Pi_{21}^1b_{11}+\Pi_{22}^1b_{21}$, $a_{22}=\Pi_{21}^1b_{12}+\Pi_{22}^1b_{22}$,
$a_{23}=\Pi_{21}^1b_{13}+\Pi_{22}^1b_{23}+\Pi_{21}^2$, $a_{24}=\Pi_{21}^1b_{14}+\Pi_{22}^1b_{24}+\Pi_{22}^2$, $a_{25}=\Pi_{21}^1b_{15}+\Pi_{22}^1b_{25}+\Pi_{25}^1$, $a_{28}=\Pi_{21}^1b_{18}+\Pi_{22}^1b_{28}+\Pi_{28}^1$,
$a_{31}=\Pi_{66}^1b_{31}$, $a_{32}=\Pi_{66}^1b_{32}$, $a_{35}=\Pi_{35}^1-\Pi_{66}^1b_{35}$, $a_{38}=\Pi_{38}^1-\Pi_{66}^1b_{38}$

$b_{11}=\frac{\Pi_{22}^0}{\Delta}$, $b_{12}=-\frac{\Pi_{12}^0}{\Delta}$, $b_{13}=\frac{\Pi_{12}^0\Pi_{21}^1-\Pi_{11}^1\Pi_{22}^0}{\Delta}$, $b_{14}=\frac{\Pi_{12}^0\Pi_{22}^1-\Pi_{12}^1\Pi_{22}^0}{\Delta}$, $b_{15}=\frac{\Pi_{25}^0\Pi_{12}^0-\Pi_{15}^0\Pi_{22}^0}{\Delta}$,
$b_{18}=\frac{\Pi_{28}^0\Pi_{12}^0-\Pi_{18}^0\Pi_{22}^0}{\Delta}$, $b_{21}=-\frac{\Pi_{21}^0}{\Delta}$, $b_{22}=\frac{\Pi_{11}^0}{\Delta}$, $b_{23}=\frac{\Pi_{11}^1\Pi_{21}^0-\Pi_{21}^1\Pi_{11}^0}{\Delta}$, $b_{24}=\frac{\Pi_{12}^1\Pi_{21}^0-\Pi_{22}^1\Pi_{11}^0}{\Delta}$,
$b_{25}=\frac{\Pi_{15}^0\Pi_{21}^0-\Pi_{25}^0\Pi_{11}^0}{\Delta}$, $b_{28}=\frac{\Pi_{18}^0\Pi_{21}^0-\Pi_{28}^0\Pi_{11}^0}{\Delta}$, $\Delta=\Pi_{11}^0\Pi_{22}^0-\Pi_{12}^0\Pi_{21}^0$, $b_{31}=\frac{1}{\Pi_{66}^0}$, $b_{32}=-\frac{2\Pi_{66}^1}{\Pi_{66}^0}$,
$b_{35}=\frac{\Pi_{35}^0}{\Pi_{66}^0}$, $b_{38}=\frac{\Pi_{38}^0}{\Pi_{66}^0}$, $J_3=J_4=2\sinh(h/2)-h\cosh(0.5)$ (A2)

in which $\Pi_{ij}^{k_1}$ interpreted as FG orthotropic shell and defined as

$$\Pi_{11}^{k_1}=\int_{-h/2}^{h/2}K_{11}(\bar{z})z^{k_1}dz,\ \Pi_{12}^{k_1}=\int_{-h/2}^{h/2}K_{12}(\bar{z})z^{k_1}dz=\int_{-h/2}^{h/2}K_{21}(\bar{z})z^{k_1}dz=\Pi_{21}^{k_1},$$
$$\Pi_{22}^{k_1}=\int_{-h/2}^{h/2}K_{22}(\bar{z})z^{k_1}dz,\ \Pi_{66}^{k_1}=\int_{-h/2}^{h/2}K_{66}(\bar{z})z^{k_1}dz,\ k_1=0,1,2$$
$$\Pi_{15}^{k_2}=\int_{-h/2}^{h/2}z^{k_2}J_1(z)K_{11}(\bar{z})z^{k_1}dz,\ \Pi_{18}^{k_2}=\int_{-h/2}^{h/2}z^{k_2}J_2(z)K_{12}(\bar{z})z^{k_1}dz,$$
$$\Pi_{25}^{k_2}=\int_{-h/2}^{h/2}z^{k_2}J_1(z)K_{21}(\bar{z})z^{k_1}dz,\ \Pi_{28}^{k_2}=\int_{-h/2}^{h/2}z^{k_2}J_2(z)K_{22}(\bar{z})z^{k_1}dz,$$
$$\Pi_{35}^{k_2}=\int_{-h/2}^{h/2}z^{k_2}J_1(z)K_{66}(\bar{z})z^{k_1}dz,\ \Pi_{38}^{k_2}=\int_{-h/2}^{h/2}z^{k_2}J_2(z)K_{66}(\bar{z})z^{k_1}dz,\ k_2=0,1 \quad \text{(A3)}$$

Appendix B

The set of Eqs. (15) contains the following coefficients

$$F_{11}=-\frac{2\alpha_1^2\left[1-e^{S_0(1-2\lambda)}\right]}{\left[(2\lambda-1)^2+\alpha_1^2\right](2\lambda-1)S_2^3}\left\{a_{12}\left[3(\lambda-1)(\lambda+1)^3+2\alpha_1^2(\lambda+4)(\lambda+1)-\alpha_1^4\right]\right.$$
$$\left.-(a_{11}-a_{31})\alpha_2^2(\lambda^2-\lambda-2+\alpha_1^2)\right\}-\frac{\left[1-e^{S_0(1-2\lambda)}\right]\alpha_1^2}{(2\lambda-1)\left((2\lambda-1)^2+4\alpha_1^2\right)S_2^3}\left\{3(2a_{31}+a_{21}-3a_{11})\alpha_2^2\right.$$
$$+(a_{11}-5a_{12}-a_{22})\left[(\lambda+1)^2(4\lambda-5)+\alpha_1^2(4\lambda+7)\right]$$
$$\left.+2(7a_{12}+4a_{22}-4a_{11}-a_{21})\left[(\lambda^2-\lambda-2)+\alpha_1^2\right]-9(a_{11}-a_{12}-a_{22}+a_{21})\right\}$$

$$F_{12}=-\frac{1}{4}\frac{\left[1-e^{2S_0(1-\lambda)}\right]\alpha_1^2}{S_2^4\left[(\lambda-1)^2+\alpha_1^2\right](\lambda-1)}\left\{-a_{13}\left[(3\lambda-4)\lambda^3+2\lambda(\lambda+2)\alpha_1^2-\alpha_1^4\right]\right.$$
$$+(a_{14}+a_{32})\alpha_2^2\left[\lambda(\lambda-2)+\alpha_1^2\right]+(4a_{14}+4a_{32}+a_{24})\alpha_2^2+(a_{23}+5a_{13}-a_{14})(2\lambda^3+2\lambda\alpha_1^2-3\lambda^2+\alpha_1^2)$$
$$\left.+(4a_{14}-4a_{23}-7a_{13}+a_{24})\left[\lambda(\lambda-2)+\alpha_1^2\right]-3(a_{14}+a_{24}+a_{32})\alpha_2^2-3(a_{23}+a_{13}-a_{14}-a_{24})\right\}$$

$$F_{13}=\frac{\left[1-e^{S_0(1-2\lambda)}\right]\alpha_1}{(2\lambda-1)\left[(2\lambda-1)^2+4\alpha_1^2\right]S_2^3}\left\{a_{35}\left[(2\lambda-1)\lambda+2\alpha_1^2\right]\alpha_2^2\right.$$
$$\left.-a_{15}\left[(2\lambda-1)\lambda^3+3\lambda\alpha_1^2-2\alpha_1^4\right]+(2a_{15}+a_{25})\left(\alpha_1^2-\lambda^2+2\lambda^3+2\lambda\alpha_1^2\right)-2a_{25}\left[(2\lambda-1)\lambda+2\alpha_1^2\right]\right\}$$
$$-\frac{\left[1-e^{S_0(1-2\lambda)}\right]\alpha_1}{(2\lambda+1)\left[(2\lambda+1)^2+4\alpha_1^2\right]S_2^3}\left\{-J_4\left[\lambda(1+2\lambda)+2\alpha_1^2\right]S_2^2+c_{35}(2\lambda+1)\alpha_2^2\right\}$$

$$F_{14}=\frac{\left(1-e^{S_0(1-2\lambda)}\right)\alpha_2}{S_2^3\left[(2\lambda-1)^2+4\alpha_1^2\right](2\lambda-1)}\left\{-2(a_{38}+a_{18})\alpha_1^2\left[(\lambda-1)\lambda+\alpha_1^2\right]-(a_{28}+2a_{18}+2a_{38})\alpha_1^2+4a_{28}\alpha_1^2\right\}$$

$$F_{21}=\frac{1}{4}\frac{\alpha_2^2\alpha_1^2\left(1-e^{-2S_0\lambda}\right)}{\lambda(\lambda^2+\alpha_1^2)S_2^2}\left[a_{21}\alpha_2^2+(a_{22}-a_{31})(\lambda^2-1+\alpha_1^2)-a_{31}+a_{22}-c_{21}\right]$$

$$F_{22}=-\frac{\left[1-e^{S_0(1-2\lambda)}\right]\alpha_1^2\alpha_2^2}{\left[(2\lambda-1)^2+4\alpha_1^2\right](2\lambda-1)S_2^3}\left\{-2(a_{32}+a_{23})\left[(\lambda-1)\lambda+\alpha_1^2\right]-2a_{24}\alpha_2^2-a_{32}-a_{23}+a_{24}\right\}$$

$$F_{23}=\alpha_1\alpha_2^2\left\{\frac{(a_{25}+a_{35})\left[(2\lambda-1)\lambda+2\alpha_1^2\right]\left[1-e^{S_0(1-2\lambda)}\right]}{\left[(2\lambda-1)^2+4\alpha_1^2\right](2\lambda-1)S_2^3}+\frac{a_{35}\left[1-e^{-2S_0\lambda}\right]}{4(\alpha_1^2+\lambda^2)S_2^2}\right\}$$

$$F_{24}=-\frac{\alpha_1^2\alpha_2}{4}\left\{\frac{\left[a_{38}(\alpha_1^2+\lambda^2)+a_{28}\alpha_2^2\right]\left(1-e^{-2\lambda S_0}\right)}{\lambda S_2^2(\alpha_1^2+\lambda^2)}+\frac{J_3\left(1-e^{-2(\lambda+1)S_0}\right)}{(\lambda+1)\left[(\lambda+1)^2+\alpha_1^2\right]}\right\}$$

$$F_{31}=\frac{1}{4}\frac{\alpha_1^2\left(1-e^{-2\lambda S_0}\right)}{\lambda\left(\alpha_1^2+\lambda^2\right)S_2^3}\left\{b_{11}\alpha_2^4+(b_{31}+b_{21}+b_{12})\alpha_2^2(\lambda^2-1+\alpha_1^2)+(2b_{31}+3b_{21}+b_{12})\alpha_2^2\right.$$
$$-(b_{31}+2b_{21}+2b_{11})\alpha_2^2+b_{22}\left[\alpha_1^2-(\lambda+1)^3(3\lambda-1)-2(\lambda+3)(\lambda+1)\alpha_1^2\right]$$
$$+(4b_{22}+b_{12}-b_{21})(2\alpha_1^2\lambda-1+3\lambda^2+3\alpha_1^2+2\lambda^3)$$
$$\left.-(5b_{22}+3b_{12}-3b_{21}-b_{11})(\alpha_1^2+\lambda^2-1)+2(b_{11}+b_{21}-b_{22}-b_{12})\right\}$$

$$F_{32}=-\frac{\left[1-e^{S_0(1-2\lambda)}\right]\alpha_1^2}{(2\lambda-1)\left[(2\lambda-1)^2+4\alpha_1^2\right]S_2^4}\left\{-2b_{14}\alpha_2^4+2(b_{32}-b_{13}-b_{24})(\lambda^2-\lambda+\alpha_1^2)\right.$$
$$-(b_{13}-2b_{32}+3b_{24})\alpha_2^2-2(b_{32}-2b_{24}-2b_{14})\alpha_2^2-2b_{23}\left[(2-3\lambda)\lambda^3-2\alpha_1^2\lambda(\lambda+1)+\alpha_1^4\right]$$
$$-(b_{13}-b_{24}+4b_{23})(4\lambda^3-3\lambda^2+4\alpha_1^2\lambda+\alpha_1^2)-2(b_{14}-3b_{13}+3b_{24}-5b_{23})\left[\lambda^2-\lambda+\alpha_1^2\right]$$
$$\left.+(b_{14}-3b_{13}+3b_{24}-5b_{23})\right\}+\frac{\left(1-e^{-2S_0\lambda}\right)\alpha_1^2\cot\gamma}{4\lambda S_2^3}$$

$$F_{33}=\frac{\alpha_1\left(1-e^{-2S_0}\right)}{4S_2^3\lambda}\left[(b_{35}+b_{15})\alpha_2^2-b_{25}(\lambda^2-\alpha_1^2)-(b_{25}+b_{15})\lambda-b_{15}\right]$$

$$F_{34}=\frac{\left(1-e^{-2\lambda S_0}\right)\alpha_1^2}{4\lambda(\alpha_1^2+\lambda^2)S_2^3}\left[b_{18}\alpha_2-b_{18}\alpha_2^3-(b_{38}+b_{28})\alpha_2(\beta_1^2+\lambda^2)\right]$$

$$F_{41}=-\frac{\alpha_1^2\left(1-e^{-2\lambda S_0}\right)\cot\gamma}{4S_2^2\lambda}$$

$$F_{43}=-\frac{\alpha_1\left[1-e^{-S_0(1+2\lambda)}\right]}{S_2\left[(2\lambda+1)^2+4\alpha_1^2\right](2\lambda+1)}\left\{J_3\left[(2\lambda+1)\lambda+2\alpha_1^2\right]+J_4(2\lambda+1)\right\}$$

$$F_{44}=\frac{2J_4\left[1-e^{-S_0(1+2\lambda)}\right]\alpha_1^2\alpha_2}{S_2(2\lambda+1)\left[2(\lambda+1)^2+4\alpha_1^2\right]},\ F_{\rho_1}=\frac{\left[1-e^{-2(1+\lambda)S_0}\right]\alpha_1^2}{4\left[(\lambda+1)^2+\alpha_1^2\right](\lambda+1)},\ F_T=-\frac{\alpha_1^2\left[1-e^{-2\lambda S_0}\right]}{4S_2^2\lambda} \quad \text{(B1)}$$